05,07

Effect of quenching on magnetostructural and magnetocaloric properties of $Mn_{0.89}Cr_{0.11}NiGe$

© V.I. Valkov[1], A.V. Golovchan[1], I.F. Gribanov[1], O.E. Kovalev[1], R.A. Safonov[1], N.Yu. Nirkov[1], A.L. Zheludkevich[2], V.I. Mitsiuk[2]

[1] Galkin Donetsk Institute for Physics and Engineering, Donetsk, Russia
[2] Scientific and Practical Materials Research Center, National Academy of Sciences of Belarus, Minsk, Belarus

E-mail: oleg_kovalev_2018@mail.ru

Received December 25, 2024
Revised April 15, 2025
Accepted April 24, 2025

The results of experimental studies of magnetic and magnetocaloric properties of quenched $Mn_{0.89}Cr_{0.11}NiGe$ samples are presented. It is shown that magnetic phase transitions from the paramagnetic to the helical state become diffuse magnetostructural phase transitions of the first order PMhex($P6_3/mmc$) $\leftrightarrow$ HMorth($Pnma$)), which is the reason for the multiple enhancement of magnetocaloric properties compared to the unquenched sample. An additional feature of quenching is the possibility of decreasing the magnetostructural transition temperature for samples with minor deviations in quenching protocols. A theoretical analysis of the merging of the diffuse first-order structural transition PMhex($P6_3/mmc$) $\leftrightarrow$ PMorth($Pnma$)) and the second-order magnetic isostructural transition PMorth($Pnma$)$-$HMorth($Pnma$)) into a single first-order magnetostructural transition PMhex($P6_3/mmc$) $\leftrightarrow$ HMorth($Pnma$)) during quenching of $Mn_{0.89}Cr_{0.11}NiGe$ is carried out. Within the framework of the model of cooperative local displacements of Ge and Ni atoms and the concept of diffuse first-order phase transitions, a theoretical description of magnetostructural transitions in slowly cooled and quenched $Mn_{0.89}Cr_{0.11}NiGe$ alloy is proposed.

Keywords: diffuse first-order phase transition, magnetocaloric effect, quenching, magnetostructural phase transition.

DOI: 10.61011/PSS.2025.04.61266.353

1. Introduction

Experimental results of alloys of the $Mn_{1-x}Cr_xNiGe$ system [1–3], show a number of common characteristic features of the magnetostructural properties. The following can be referred as the most important among them: (1) a significant difference in the temperatures of structural and magnetic phase transitions for samples slowly cooled after homogenizing annealing (850 °C). In this case, blurred structural transitions of the 1st order displacement PMhex $\leftrightarrow$ PMorth [3,4] between hexagonal hex (symmetry group $P6_3/mmc$) and orthorhombic (symmetry group $Pnma$) paramagnetic (PM) phases exceed by more than 100 K the temperature of the isostructural magnetic phase transition of the 2nd order from paramagnetic to helimagnetic (HM) phase PMorth $\leftrightarrow$ HMorth; (2) convergence (to alignment) of the structural and magnetic transitions for samples subjected to hydrostatic pressure or quenched after prolonged homogenizing annealing (850 °C) in ice water. For example, the lability (absolute instability) temperatures of the structural transitions of the 1st order PMhex $\leftrightarrow$ PMorth (T_{t2}, $T_{t1} < T_{t2}$) decrease from 470 to 370 K and from 430 to 380 K (for T_{t1}) for quenched NiMnGe and $Mn_{0.93}Cr_{0.07}NiGe$ samples, respectively [1]. This significantly shortens the temperature interval between the structural transitions of 1st order PMhex $\leftrightarrow$ PMorth and the isostructural magnetic phase transitions of 2nd order PMorth $\leftrightarrow$ HMorth.

A theoretical description of the magnetostructural and magnetocaloric properties of the semi-Heusler alloys of $Mn_{1-x}Cr_xNiGe$ system is given in Refs. [3,4]. In general, only slowly cooled alloys were described, in which the temperature-differentiated blurred structural transition of 1st order of displacement type PMhex $\leftrightarrow$ PMorth and isostructural magnetic phase transition of 2nd order from paramagnetic to helimagnetic state PMorth$-$HMorth are realized in $x \leq 0.18$ and, in particular, in $Mn_{0.89}Cr_{0.11}NiGe$. The authors assumed in Refs. [3,4], that slow cooling of the sample from the homogenizing annealing temperature (850 °C) leads to the realization of the equilibrium pretransition hexagonal PMhex phase with a stable configuration of atoms in the Ni and Ge sublattices (the Ni positions are occupied only by Ni atoms, the Ge positions are occupied only by Ge atoms). The helimagnetic ordering is realized in the orthorhombic phase below the Neel temperature ($T < T_N$) [6] in the spin subsystem according to Ref. [5]. It is understood that the substitution atoms (Cr) in the Mn sublattice can form such a stable configuration in

case of slow cooling that ensures [7] a minimum distance between the Mn atoms and, consequently, a maximum magnetic ordering temperature.

The present paper is devoted to the presentation and discussion of the experimental results of magnetic, X-ray and magnetocaloric properties of independently prepared quenched samples of $Mn_{0.89}Cr_{0.11}NiGe$, in which blurred magnetostructural transitions of the 1st order PMhex $\leftrightarrow$ HMorth with low characteristic temperatures are realized. The theoretical analysis of the magnetocaloric effect in the studied samples is also carried out in this work. The calculations were carried out in the framework of the model of local structural mode [2,8,9] under the condition of its softening and subsequent freezing in homogeneous nuclei of heterogeneous magnetically active medium [3,4,10].

2. Methods for the preparation and measurement of samples

The studied samples were prepared by induction melting of the starting elements Mn, Cr, Ni, Ge taken in appropriate proportions. The starting material suspensions were twice remelted by induction melting in a sealed evacuated quartz ampoule, then annealed in a furnace in a vacuum environment at 850 °C for 110 h and slowly cooled with the furnace (slowly cooled samples — s). Then one part of the obtained ingot was again placed in an evacuated quartz ampoule and heated to an annealing temperature of 850 °C and, it was quenched after holding for 3 h by rapid transferring the ampoule to water and then breaking it (quenched samples — z). The elemental composition of the samples obtained is given in Table 1.

The temperature dependences of the magnetization $M(T)$ in a constant magnetic field up to 0.97 T were measured on Domenicali type pendulum magnetic scales. The magnetocaloric properties of the sample were evaluated indirectly by estimating the isothermal entropy change $\Delta S^M(T)_{\Delta H}$ from the temperature dependences of magnetization in different magnetic fields using Maxwell's relation

$$\Delta S^M(T)_{\Delta H} = \int_0^{H_0} \left(\frac{\partial M}{\partial T}\right)_H dH. \qquad (1)$$

The set of isofield temperature dependences of the magnetization $M(T)$ was rearranged into a set of isothermal field dependences $M(H)$ for calculating the magnetocaloric effect by relationship (1). This approach allows for a correct calculation of the magnetocaloric effect in the hysteresis region of the blurred phase transition of the 1st order.

3. Experimental results

This paper presents the results of two samples of $Mn_{0.89}Cr_{0.11}NiGe$ composition prepared independently.

Table 1. Elemental analysis of slowly cooled samples $Mn_{0.89}Cr_{0.11}NiGe$

Batch № 1		Batch № 2
Element	at.%	at.%
Ge K_α	32.71	33.56
Ni K_α	33.55	33.13
Mn K_α	29.71	29.17
Cr K_α	4.03	4.14
Total	100	100

Elemental analysis of the obtained samples (see Table 1) shows that their composition is almost identical. The temperature dependences of the inverse paramagnetic susceptibility $\chi(T)^{-1}$ of slowly cooled samples show anomalous behavior characteristic of the structural transition 1st order PMhex $\leftrightarrow$ PMorth. The main features of these anomalies are the splitting of the inverse susceptibility into two branches and the appearance of temperature hysteresis (Figure 1).

Each of the branches on either side of the temperature hysteresis region describes the inverse susceptibility of the spin subsystem $\chi_{hex}(T)^{-1}$, $\chi_{orth}(T)^{-1}$ in the hexagonal or orthorhombic phase, respectively. At the same time, the temperature region of anomalous changes $\chi(T)^{-1}$ determined by the intervals of the lability temperatures $\delta T_{t2}, \delta T_{t1}$ of the corresponding phases PMorth, PMhex (Figure 1, a, Figure 2, a) is almost 80 K higher than the temperature of smooth magnetization growth. Since the corresponding paramagnetic Curie temperatures are related as $\theta_{orth} \gg \theta_{hex}$ (Figure 1, a, Figure 2, a), then magnetic ordering in the spin subsystem in the slowly cooled samples is induced by a structural phase transition. This transition is realized as a magnetic phase transformation of the 2nd order PMorth−HMorth at the Neel temperature $T_N \geq \theta_{orth}$. The structural transition of the 1st order PMhex $\leftrightarrow$ PMorth, as the reason for the shift of magnetic ordering to the higher temperature region ($T_N \gg \theta_{hex}$), can be qualified as a blurred 1st order transition, which is directly confirmed by the course of the temperature dependence of the intensity X−Int$_{orth}(T)$ of the diffraction peak of the orthorhombic phase (Figure 1, b, Figure 2, b). No appreciable change in X−Int$_{orth}(T)$ of the orthorhombic phase in the region of the magnetic phase transition is observed, which confirms the isostructural nature of magnetic ordering (i. e., magnetic ordering does not break the orthorhombic symmetry).

Completely different results are obtained from measurements of two independently prepared quenched specimens. First, according to Figures 1, a, and 1, b, there are no anomalous regions on the temperature dependences $\chi(T)^{-1}$ responsible for the separation of $\chi(T)^{-1}$ into two branches. Therefore, it is possible to state the existence of only paramagnetic branch of $\chi_{hexz}(T)^{-1}$ for the quenched samples.

The paramagnetic Curie temperatures in this case are in the relation $\theta_{hexz2} < \theta_{hexz1}$.

Second, magnetic ordering is realized in each of the quenched samples as a blurred magnetostructural transition of the 1st order PMhex $\leftrightarrow$ HMorth. This is clearly demonstrated by the temperature dependences of the magnetization $Mz1(T)$, $Mz2(T)$, which possess temperature hysteresis and are accompanied by a change in the ratio between the content of competing phases $Xz1(T)$, $Xz2(T)$ (see Figure 1, *c, b*, Figure 2, *c, b*).

The isothermal field dependences $Mz1(H)$, $Mz2(H)$ measured in a stationary magnetic field on a vibrating magnetometer (Figure 3, *a* and 3, *b*) provide insights not only into the saturation magnetization values of the quenched samples, but also demonstrate the field-induced transitions. Thus, the dependences $Mz1(H)$, $Mz2(H)$ at $T = 278$ K and $T = 240$ K shown in Figure 3, *a* and Figure 3, *b*, respectively, are accompanied by field hysteresis and a sharp change in the magnetization value in a relatively narrow range of magnetic fields. This allows defining the critical field of the induced transition and to separate the initial and induced states. This behavior is characteristic of the magnetic field induced transitions of the 1st order [11,12] (in the present case — magnetostructural blurred transitions

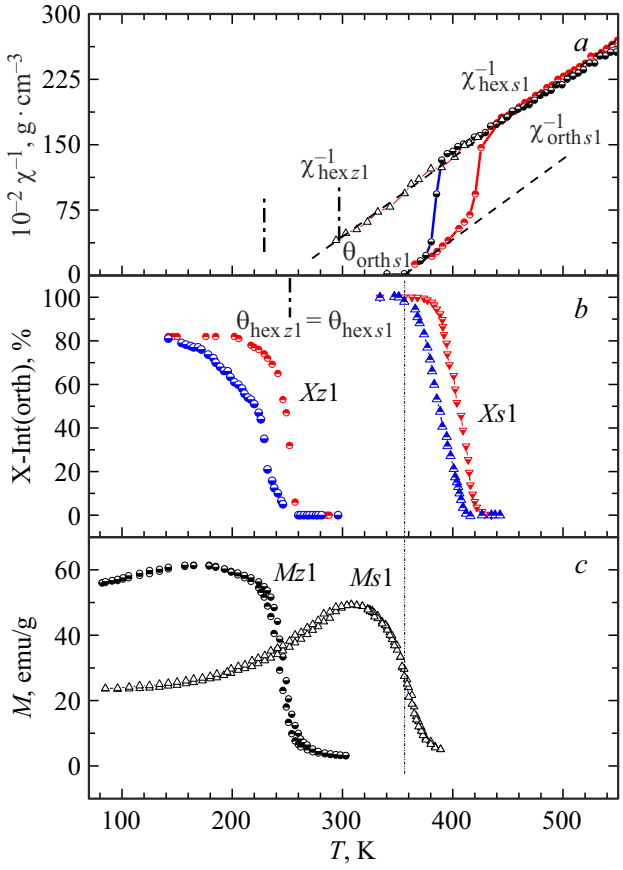


Figure 1. Temperature dependences of the magnetostructural characteristics of slowly cooled (s) and quenched (z) samples from batch № 1.

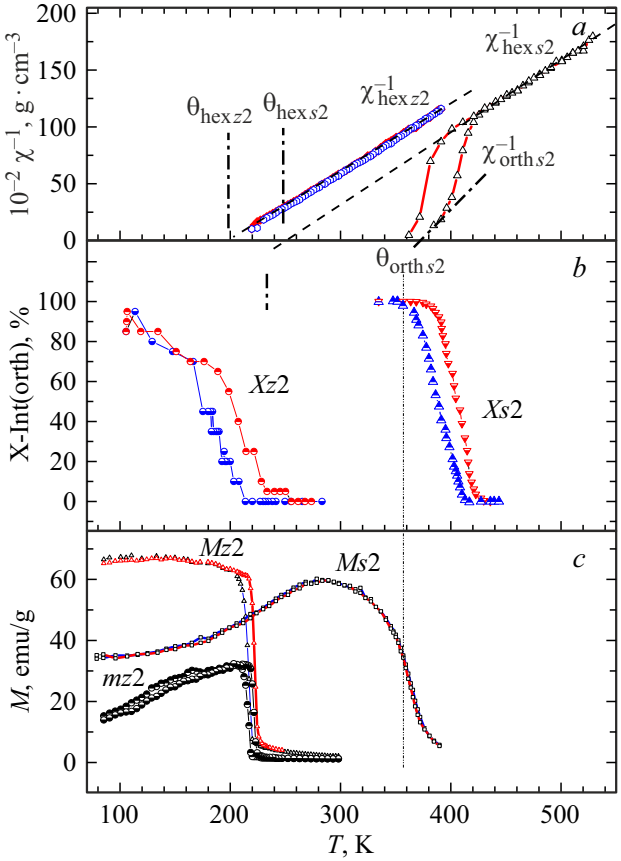


Figure 2. Temperature dependences of magnetostructural characteristics of slowly cooled (s) and quenched (z) samples from batch № 2.

of the 1st order PMhex $\leftrightarrow$ FMorth). The field dependences show a smooth magnetization of the initial helicoidal state to the saturation state of the collinear phase at lower temperatures.

Temperature dependences of the isothermal entropy change $\Delta S^M(T)_{\Delta H}$ (Figure 3) are plotted on the basis of the field dependences (Figure 4) using the Maxwell (1) relation. As can be seen from the figure, in independently prepared samples of the same composition, the temperatures of the maximum of the magnetocaloric effect differ by 40 K, and the magnitude of ΔS differs by only 16 % (49 J/kg · K vs. 57 J/kg · K) when the magnetic field changes from 0 to 8 T.

The differences in magnetic and magnetocaloric properties between the slowly cooled and quenched samples are evident in Figure 5. The main qualitative and quantitative features due to quenching are clearly shown here. Qualitative features include: change in the character of magnetic ordering: from isostructural magnetic phase transitions of the 2nd order PMorth $\leftrightarrow$ HMorth to blurred magnetostructural phase transitions of the 1st order PMhex $\leftrightarrow$ HMorth. Quantitative features are expressed in the multiple increase of magnetocaloric effect (MCE) values for quenched (z) samples (Figure 5, *b*) with a significant decrease in the characteristic temperatures of the magnetostructural phase

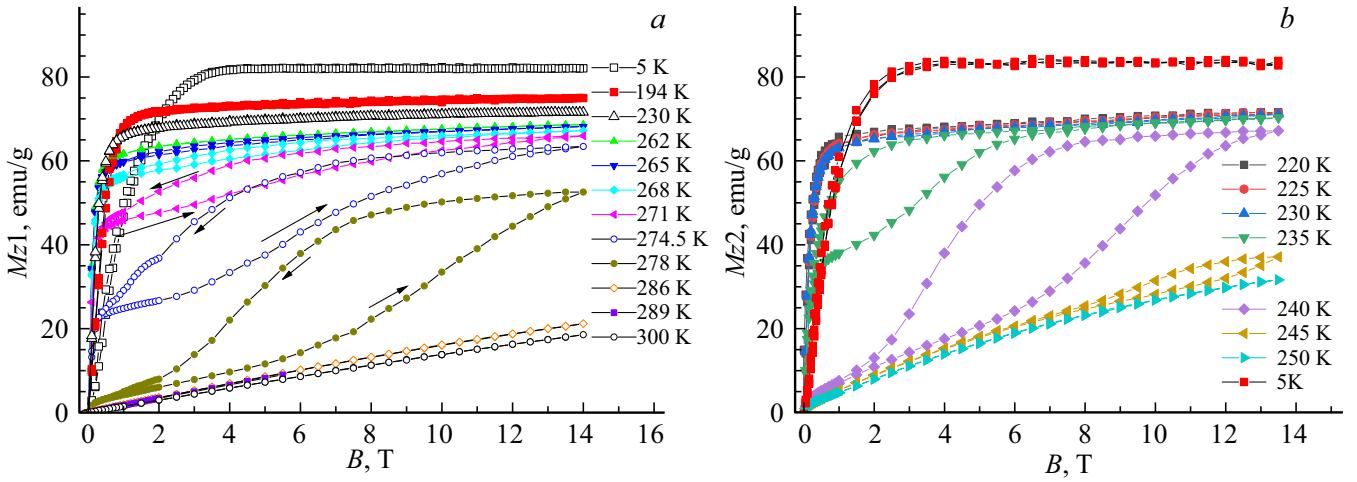


Figure 3. Isothermal field dependences of the magnetization $Mz1(H)$, $Mz2(H)$ of independently prepared and independently quenched samples № 1 and № 2.

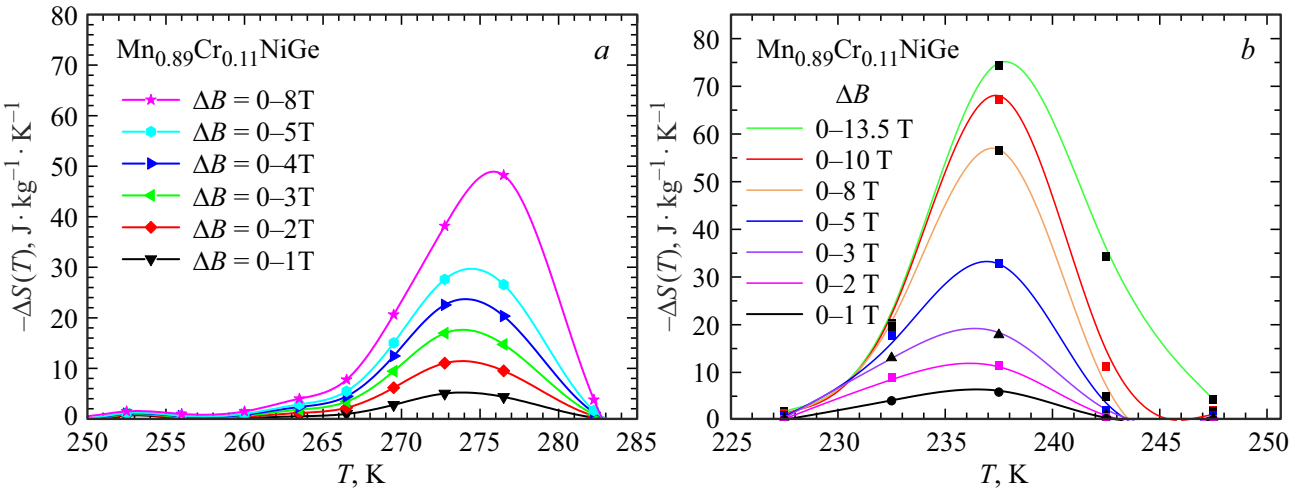


Figure 4. Temperature dependences of magnetic entropy for independently prepared and independently quenched samples of № 1 (a) and № 2 (b) of $Mn_{0.89}Cr_{0.11}NiGe$ composition in case of heating.

transition. At the same time, the Neel temperatures $T^{s1,s2}_{\text{Nheatimg}} = T^{s1,s2}_{\text{Ncooling}}$, determined from the positions of the maxima of the maximums of the temperature dependence of the magnetic entropy $\Delta S(T)$ for slowly cooled (s) and quenched (z) samples of the first (1) and second (2) batches is in the following relationship:

$$T^{s1,s2}_{\text{Nheatimg}} = T^{s1,z2}_{\text{Ncooling}} \approx 350\,\text{K} > T^{z1}_{\text{Nheatimg}}$$
$$\approx 270\,\text{K} > T^{z2}_{\text{Nheatimg}} \approx 225\,\text{K}.$$

One of the main problems in estimating the change in the magnetic part of the entropy in the neighborhood of 1st order phase transitions from magnetic measurements using Maxwell's relation is to correctly account for the hysteresis region. Isopole temperature dependences of magnetization are taken as a basis in this study, which makes it possible to avoid „early" induction of the high-magnetic phase both during heating and cooling. The resulting set of isofield curves $M(T)$ for the calculation of $\Delta S(T)$ is rearranged into a set of isothermal field dependences $M(H)$, which allows comparing the results with literature data. The results of such a calculation procedure $\Delta S(T)$ for heating (h), cooling (c) of the sample are shown in Figure 5. It should be noted that when heated, this method of calculating $\Delta S(T)$ gives identical results to the direct use method $M(H)$. But it becomes advantageous when cooling samples possessing a metastable temperature region (temperature hysteresis at 1st god transitions), since it initially contains a return to initial conditions (paramagnetic state). This eliminates the „start" of dependencies $Mz1(H)$, $Mz2(H)$ from irreversibly induced states [12] that persist after previous magnetization in the temperature hysteresis region.

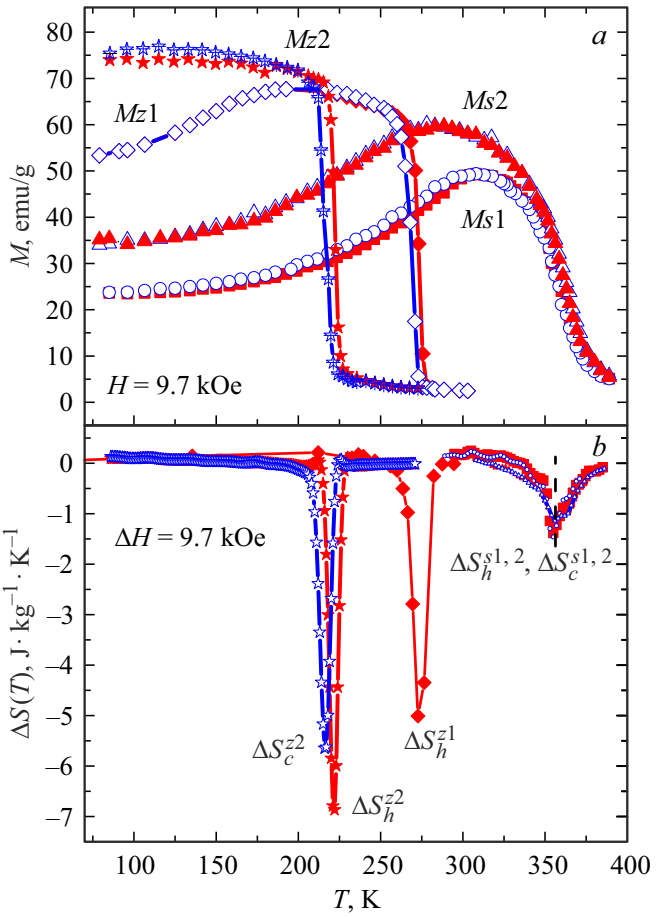


Figure 5. Comparison of magnetic and magnetocaloric characteristics of slowly cooled $(s1, s2)$ and quenched $(z1, z2)$ samples. Red lines — heating, blue lines — cooling. Asterisks correspond to the data for the quenched sample from batch № 2, rhombuses correspond to the data for quenched sample from batch № 1, triangles correspond to the data for slowly cooled sample from batch № 2, circles correspond to the data for slowly cooled sample from batch № 1.

4. Hardening of alloys of the $Mn_{1-x}Cr_xNiGe$ system in framework of the local cooperative displacement model

In constructing the model of structural transitions of the 1st order, we will assume that the soft mode responsible for the structural transition in $Mn_{1-x}Cr_xNiGe$ system corresponds to the local optical mode (soft mode) of the hexagonal phase (cf. Figure 6, *a*) which is reduced to a combination of local displacements of pairs of Ni and Ge atoms $(U_{nz}^{Ni1} - U_{nz}^{Ni2})/2a = Q_{nz}$, $(U_{nx}^{Ge1} - U_{nx}^{Ge2})/2c = Q_{nx}$ (Figure 6, *b*). The average (in time) values of these quantities are equal to zero $(\langle Q_{nz}\rangle = \langle U_{nz}^{Ni1,2}\rangle = \langle Q_{nx}\rangle = \langle U_{nx}^{Ge1,2}\rangle = 0)$ at finite temperatures in the hexagonal phase. Freezing of the soft mode at a certain temperature leads to static local displacements of Ni and Ge atoms to a new equilibrium position. The implication is that the new equilibrium positions of the Ni and Ge atoms lead to nonlocal displacements of the Mn atoms and a structural transition to the orthorhombic PMorth phase.

A combined approach is used in this paper to describe the above structural transitions in the general case (slowly cooled samples $Mn_{0.89}Cr_{0.11}NiGe$) and rapidly quenched samples in particular. Three subsystems are considered for a homogeneous medium consisting of N_0 elementary hexagonal cells: structural (Q), spin (s), and elastic (e). Such a homogeneous medium and its magnetostructural properties are assumed to be characteristic of the germ space of $g \ll N_0$ structural units (lattice cells) of the heterogeneous medium.

The magnetostructural properties of the homogeneous system were described in Refs. [2,9] based on the full thermodynamic potential (TP) Ω (see Appendix):

$$\Omega \equiv \Omega(Q_0, y, e_1, e_2) = \Omega_e(e_1, e_2) + \Omega_s(Q_0, y, e_1) + \Omega_Q(Q_0, e_1, e_2). \quad (2)$$

$Q_0 = \langle Q_{nz}\rangle$, $y = \langle \hat{s}_n^k\rangle/s$ are nonequilibrium parameters of structural and magnetic orders (see Appendix) in expression (2), e_1, e_2 are elastic strains describing volume change and orthorhombic distortion (Figure 6). The thermodynamic potential $\Omega_Q(Q_0, e_1, e_2)$ of the structural subsystem, in which the structural transition from hexagonal to orthorhombic phase is described by the microscopic Hamiltonian (A1), was calculated in the shifted harmonic oscillator approximation. The spin subsystem in which the helicoidal structure with wave vector $\mathbf{q} = [0, 0, q_a]$ arises is described by the Hamiltonian (A2). The thermodynamic potential of the spin subsystem $\Omega_s(Q_0, y, e_1)$ is calculated in the space-periodic mean-field approximation $\mathbf{h}_n^k = h\mathbf{U}_n^k \equiv h(\mathbf{q})\mathbf{U}_n^k(\mathbf{q})$. The direction of the mean field for the kth atom Mn in the nth lattice cell in the presence of an external magnetic field $\mathbf{H}_0 = [0, 0, H_0]$ is determined by the unit vector $\mathbf{U}_n^k(\mathbf{q})$ (see Appendix). The relation between the magnetic order parameter y and the uniform magnetization M of the spin half-system in a magnetic field $\mathbf{H}_0 = [0, 0, H_0]$ is described by the relation

$$M = M_0(s) y \cos(\vartheta), \quad (3)$$

where $\vartheta \equiv \vartheta(H_0, Q_0)$ is the angle between the directions $\mathbf{H}$ and $\mathbf{h}_n^k$.

The bulk elastic deformations $e_1 = e_{xx} + e_{yy} + e_{zz}$ and deformations in the basis plane (xy) $e_2 = (e_{xx} - e_{yy}) = (c/b - \sqrt{3})/\sqrt{3}$ of the lattice cell are described by the TP of the elastic subsystem $\Omega_e(e_2, e_1)$:

$$\Omega_e(e_2, e_1) = \frac{1}{2} e_1^2 k_0 + \frac{1}{2} k_1 (e_2)^2 + P e_1 - T(v_0 e_1), \quad (4)$$

where e_{ii} are the elastic strains along the corresponding axes; strains e_2 describing distortions of the orthorhombic cell as a whole arise from optical displacements of Ni and Ge atoms (Figure 6) and act as secondary order parameters.

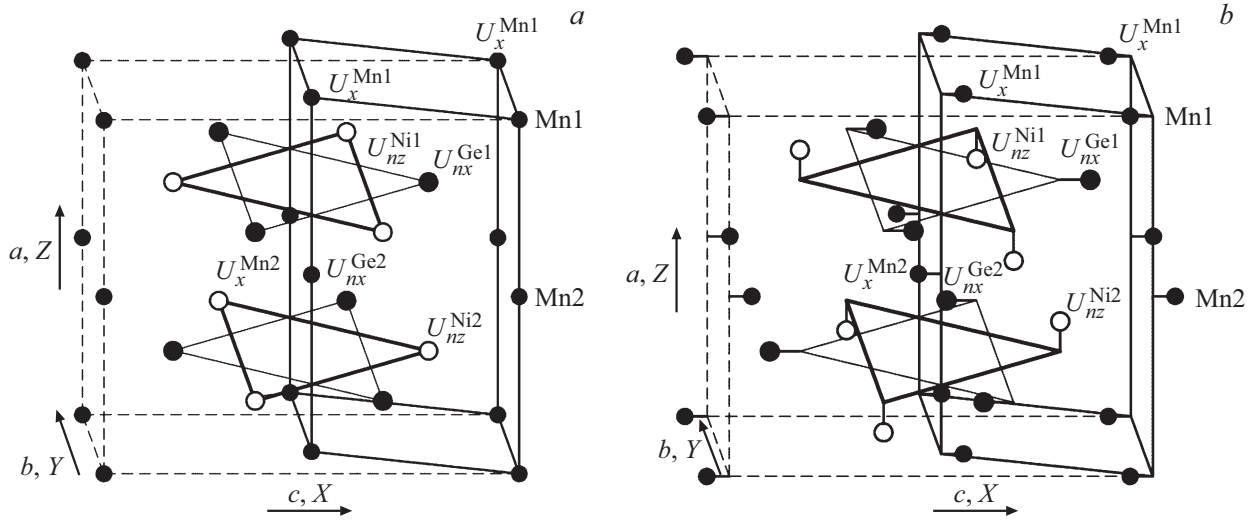


Figure 6. Structural transitions of the „displacement" type in MnNiGe: *a* — high-temperature pre-transition hexagonal phase hex($P6_3/mmc$), lattice cell is highlighted by bold lines; *b* — low-temperature orthorhombic phase orth($Pnma$), the lattice cell indicated by dashed lines is characterized by displacements of Ni, Ge, Mn atoms and orthorhombic distortions ($e_2 = (c/b - \sqrt{3})/\sqrt{3} \neq 0$).

Equilibrium value of magnetization

$$M(H_0, T) \equiv M\big(H_0, y(T), Q_0(T)\big)$$

is determined by the equilibrium values of the magnetic and structural order parameters, which are solutions of the system of equations of state

$$(\partial\Omega/\partial Q_0) = 0, \quad (\partial\Omega/\partial y) = 0,$$
$$(\partial\Omega/\partial\sigma) = 0, \quad (\partial\Omega/\partial e_1) = 0,$$
$$(\partial\Omega/\partial e_2) = 0, \quad (\partial\Omega/\partial\vartheta) = 0. \qquad (5)$$

The transition from the hexagonal paramagnetic (PM) state PMhex to the orthorhombic paramagnetic state PMorth at decreasing temperature is associated in the framework of the outlined approach with the appearance of a nonzero solution $Q_0 \equiv Q_0(T)$ of equations $(\partial\Omega/\partial Q_0) = 0$, $(\partial\Omega/\partial\sigma) = 0$. This solution, called the equilibrium solution, results from the competition between the intracellular $V(Q_0, \sigma)$ and intercellular $-\frac{1}{2} N_0 \nu_0(e_1, e_2) Q_0^2$ energies (A1, A5b). TP Ω_Q describes bias-type transitions with one-minimum potential $V(Q_0, \sigma)$ at $\omega_0^2 > 0$, $\gamma > 0$, $\Gamma > 0$ [8]. It should be noted also that if the applicability condition of the shifted harmonic oscillator approximation $\omega^2 < \nu_0 < 2\omega^2$ and weak interactions with the elastic subsystem is satisfied, this transition will be a smooth hysteresis-free transition of the 2nd order, which is typical of structural phase transitions of the 2nd order of displacement type. Under strong structural-elastic interactions, this transition can become a transition of the 1st order with discontinuous changes in the structural order parameter, elastic strain values, and different lability temperatures for the hexagonal T_{t1} and orthorhombic $T_{t2} > T_{t1}$ phases. In the simple case, when $\Gamma = 0$, the value of T_{t1} is determined by expression (6a). The paramagnetic Curie temperature θ_{hex} of the spin subsystem in the hexagonal phase is determined by expression (6b)

$$T_{t1} = \frac{1}{3k_B\gamma}\,\tilde{\nu}_0(\tilde{\nu}_0 - \omega^2),$$

$$\tilde{\nu}_0 = \nu_0(1 + L_2 e_1 + L_3 e_2) = \sum_n \nu_{nn'}, \qquad (6a)$$

$$\theta_{\text{hex}} = T_0(1 + 3z), \qquad (6b)$$

where

$$\tilde{\nu}_0 = \nu_0(1 + L_1 e_1 + L_2 e_2), \;\; e_1 \equiv e_1(Q_0 = y = 0),$$

$$e_2 \equiv e_2(Q_0 = 0), \;\; T_0 = J_{00}\, s(s+1)2/3k_B,$$

J_{00}, z — Fourier component parameters of the exchange interaction integrals in the ferromagnetic hexagonal state $J(\mathbf{q} = Q_0 = 0)$; $s = 3/2$ (see Appendix). According to (6a), by varying the value ω within $\omega^2 < \nu_0 < 2\omega^2$ it is possible to vary the temperature T_{t1} and also the temperature T_{t2}. Two limiting cases are of interest in this case:

1) $T_{t1} > \theta_{\text{orth}} > \theta_{\text{hex}}$. T_{t1} exceeds the paramagnetic (PM) Curie temperature of the orthorhombic phase (θ_{orth}) and is significantly larger than the $T_{t1} \gg \theta_{\text{hex}}$ PM Curie temperature of the hexagonal phase (θ_{hex}). This case is characteristic of slowly cooled $Mn_{0.89}Cr_{0.11}NiGe$ samples, in which the helicoidal ordering temperature T_N is in the following ratio with other characteristic temperatures $T_{t1} > T_N \geq \theta_{\text{orth}} > \theta_{\text{hex}}$.

2) $T_{t1} \cong \theta_{\text{orth}} > \theta_{\text{hex}}$. In the framework of the model of point (jump) transitions of the 1st order, this case can be applied to the description of single magnetostructural transitions of the 1st order PMhex $\leftrightarrow$ PMorth, observed in rapidly quenched samples $Mn_{0.89}Cr_{0.11}NiGe$.

Thus, the different magnetostructural behaviors of the samples given in the previous section can be understood from the position of the point model under the following assumptions.

1. The most optimal configuration of Ni and Ge atoms, in which each atom occupies its own positions, has time to form and stabilize in case of slow cooling of the image in the pre-transition region of the hexagonal phase. It is assumed that in this case the maximum value of the lability temperatures of the structural transition PMhex $\leftrightarrow$ PMorth is reached and the condition $T_{t1} > T_N \geq \theta_{orth} > \theta_{hex}$ and $T_{t1} \gg \theta_{hex}$ is realized for $Mn_{0.89}Cr_{0.11}NiGe$, which ensures the temperature separation of the structural transition of the 1st order PMhex $\leftrightarrow$ PMorth and the isostructural magnetic transition of the 2nd order PMorth$-$HMorth.

2. The quenching under rapid cooling from temperature 850 °C can lead to the conservation of one of the metastable configurations of the pre-transition hexagonal state. The distribution of Ni and Ge atoms in positions is more chaotic for metastable fluctuating configurations, which, from the position of the point model of structural transitions, leads to a less optimal ratio between the parameters of intercellular and intracellular interactions and, as a consequence, to a decrease in the lability temperatures of the structural transition T_{t1} until approaching the paramagnetic Curie temperature θ_{orth} of the orthorhombic phase $T_{t1} \geq \theta_{orth} > \theta_{hex}$. In this case the magnetic ordering processes in the spin subsystem are involved in the processes of structural rearrangement in the structural subsystem. The alignment of both processes leads to a single magnetostructural transition of the 1st order PMhex $\leftrightarrow$ HMorth.

It is also necessary to note the possibility of a less-than-optimal distribution pattern of Mn and Cr atoms from the perspective of the probabilistic formation model of the shortest distance between atoms Mn [7]. This can also lead to a decrease in the magnitude of θ_{hex} and even a change in the type of magnetic order [7].

5. Blurred structural transitions of the 1st order

The transition to a more realistic description of structural phase transitions as blurred structural transitions of the 1st order is carried out in this study according to the scheme proposed in Refs. [3,4]. In the model of blurred transitions, the equilibrium values of the magnetic and structural order parameters calculated from the equations of state (4) are transformed to the following order $x \leq 0.18$

$$y^*_{c,h}(T) = y(T)L_{1c,h}(T), \tag{7a}$$

$$Q^*_{0c,h}(T) = Q_0(T)L_{1c,h}(T), \tag{7b}$$

where $L_{1c,h}(T)$ is the relative number of orthorhombic phase nucleates in the heterogeneous state of the system under cooling (c), heating (h). It is suggested that the dependencies $L_{1c,h}(T)$ may be associated with the temperature dependence $X-Int_{orth}(T)$ [3,4], describing the relative change of the orthorhombic phase content in the sample in the region of the paramagnetic structural transition of the 1st order PMhex $\leftrightarrow$ PMorth. In the case of non-interacting nuclei, when the change in the ratio between the relative numbers of nuclei of orthorhombic (L_1), hexagonal (L_2) phase $L_1, L_2 = 1-L_1$ will be caused by the mixing entropy [10]:

$$\begin{aligned} S &= -k_B[L_1 \ln L_1 + L_2 \ln L_2] \\ &\equiv -k_B[L_1 \ln L_1 + (1-L_1)\ln(1-L_1)]. \end{aligned}$$

The dependence $L_1(T)$ is reduced to the following order [3]

$$L_{1c,h}(T) = \left(1 + e^{(\Delta U^{c,h}_{12})/(k_B T)}\right)^{-1}, \tag{8a}$$

$$\Delta U^{c,h}_{12} = \left(\frac{\Omega_1 - \Omega_2}{N_0}\right)g + g^{2/3}\left(\frac{n^{c,h}_1\Omega_1 - n^{c,h}_2\Omega_2}{N_0}\right), \tag{8b}$$

$$\Omega_1 = \Omega(\text{orth}) \equiv \Omega(Q_0, y, e_1, T, P, H),$$

$$\Omega_2 = \Omega(\text{hex}) \equiv \Omega(Q_0 = 0, y, e_1, T, P, H), \tag{8c}$$

where $Q_0 \equiv Q_0(T)$, $y \equiv y(T)$, $e_1 \equiv e_1(T, P, y, Q_0)$, $e_2 \equiv e_2(Q_0)$ — the corresponding equilibrium functions of structural, magnetic order, bulk, and orthorhombic strain parameters calculated from solutions of the equations of state (4) in the point transition model [2] $\Omega(Q_0, y, T, P, H) \equiv \Omega_1$ and $\Omega(Q_0 = 0, y, T, P, H) \equiv \Omega_2$ — equilibrium TPs calculated for the orthorhombic and hexagonal phases, respectively.

Thus, the model of blurred structural transitions of the 1st order used combines two approaches: a semi-microscopic model of point jump transitions for a homogeneous nucleation medium and a thermodynamic model of nucleation mixing of competing phases for a heterogeneous medium arising in the vicinity of real transitions of the 1st order.

The model was validated by describing the magnetostructural properties of slowly cooled $Mn_{0.89}Cr_{0.11}NiGe$ alloys. At this stage, the main model parameters responsible for the characteristic temperatures of the spaced structural and magnetic transitions at atmospheric pressure were selected (see Figure 7). Such parameters primarily include the parameters of intercell $(\nu_0(1 + L_2e_1 + L_3e_2))$, intracell (ω, γ, Γ) interactions; parameters $A, \tilde{A}, B, \tilde{B}$ and T_0 responsible for the helicoidal structure characteristics and the paramagnetic Curie temperature θ_{hex} (Figure 7, *a*). The parameters $n^{c,h}_1$ and $n^{c,h}_2$ (8b) complement this set. The parameters selected for describing the magnetostructural properties at atmospheric pressure were kept as a reference and did not change with pressure changes. A satisfactory description of the baric effects was an additional verification of the choice of parameters. The sets of the most important model parameters are summarized in Table 2 for describing the properties of the samples during slow cooling and their modified values used to describe the effects of rapid quenching.

Figure 7 shows the combined experimental and model dependences, which give an idea of the most characteristic

Table 2. Main model parameters for describing the properties of slowly cooled and quenched samples $Mn_{0.89}Cr_{0.11}NiGe$. Calculations were performed for $\tilde{A} = \tilde{B} = 0$

$\sqrt{N_0}\omega$, $\sqrt{\text{kbar}}$	$N_0\nu_0$, kbar	$N_0\gamma$, kbar	M_0, emu/g	M_{00}, emu/g	λ_{00}	α, K^{-1}	κ, 1/kbar	A/B	z	T_0, K	g	$\cos(\Psi)$
Slowly cooled												
4.455	38.976	134.3	80.2	100	24	$5 \cdot 10^{-5}$	$2 \cdot 10^{-3}$	9/150	1.265	47	190	0.88−0.884
Rapidly quenched1												
6.597	38.976	134.3	80.2	133.75	24.6	$5 \cdot 10^{-5}$	$2 \cdot 10^{-3}$	11/200	1.265	44	100	0.89−0.906
Rapidly quenched2												
7.283	38.976	134.3	80.2	133.75	24.6	$5.0 \cdot 10^{-5}$	$2 \cdot 10^{-3}$	19.5/980	1.265	42	100	0.877−0.965

features of the magnetostructural properties of slowly cooled $Mn_{0.89}Cr_{0.11}NiGe$ samples and allow evaluating the adequacy of the model provisions used. As can be seen from Figure 6, *a*, the anomalous splitting of the temperature dependence of the inverse susceptibility $\chi(T)^{-1}$ into hexagonal $\chi_{\text{hex}}(T)^{-1}$ and orthorhombic $\chi_{\text{orth}}(T)^{-1}$ branches demonstrate a good qualitative agreement between the initial model assumptions and experimental realities of the blurred structural transition of the 1st order PMhex $\leftrightarrow$ PMorth (in further paramagnetic structural transition of the 1st order).

The analytical expression for the model dependence $\chi(T)^{-1}$ allows understanding the mechanism of formation of the anomalous transition region $\chi(T)^{-1}$ and estimating the value $\Delta\chi(T)^{-1} = \chi_{\text{hex}}(T)^{-1} - \chi_{\text{orth}}(T)^{-1}$ (see Figure 7, *a*). It turns out that $\Delta\chi(T_{t1})^{-1} \propto Q_0^*(T_{t1})^{10/9}$ (see Figure 7, *d*). The change in the phase ratio (temperature dependence of the reflex intensity [211] of the $X-\text{Int}_{\text{orth}}(T)$ orthorhombic phase at Figure 7, *b*), demonstrates the fuzzy PM character of the 1st order structural transition and is successfully modeled by the theoretical dependencies $L_{1c,h}$ (8a). These dependences and theoretical temperature dependences of the structural order parameter $Q^*_{0c,h}(T)$ show that helimagnetic ordering is realized in the stability region of the orthorhombic state as a result of a hysteresis-free smooth isostructural phase transition of the 2nd order PMorth−HMorth (Figure 7, *c*). This transition, separated by more than 100 ° from the blurred structural transition of the 1st order PMorth $\leftrightarrow$ PMhex, is accompanied by a characteristic temperature dependence of the magnetization $M(T)$ with a maximum $M(T_{\max})$ at $\theta_{\text{hex}} < T_{N_{\text{orth}_{\max}}}$. The model dependence (Figure 7, *c*) of the helimagnetic state magnetization $M(T) = M_0(x)y^* \cos\big(\theta(T, H, y^*)\big)$ was calculated for the case $\mathbf{H} \parallel \mathbf{q} = [0, 0, q_a]$. $M_0(x)$ is the maximum magnetic moment at collinear configuration $\big(\cos\vartheta(T) = 1\big)$ localized spins of Mn for the sample c given x and spin $s = 3/2$. Let us use the following expression for its calculation

$$M_0[\text{emu/g}] = (1-x)2s\mu_B/A(x) = 1.116906s \cdot 10000(1-x)/A, \qquad (9)$$

where $A(x)$ is the atomic weight per formula unit.

The coupling between the structural and magnetic subsystems arising in the slowly cooled sample ensures that the inequality $\theta_{\text{hex}} \ll \theta_{\text{orth}}$ is satisfied, but does not change the nature of the magnetic ordering. The isostructural magnetic phase transition PMorth−HMorth is realized as a phase transformation of the 2nd order. Presumably, spin-structure and structure-elastic interactions, as well as spin-elastic interactions, lead to the characteristic $P-T$-diagram of states (see Figure 8, *a*). By considering the dependence of the Fourier component of the mean field $h(\mathbf{q})$ (8b) in the spin subsystem on the structural order parameters and bulk strain e_1 in the form $h(\mathbf{q}) \equiv h(Q_0^{*10/9}, e_1Q_0^{*10/9}, Q_0^{*2}, Q_0^{*4})$, and the dependence $\tilde{\nu}_0 = \nu_0(1 + L_1e_1 + L_2e_2)$ in the structural subsystem, the model $P-T$-diagram (Figure 8, *b*) agrees with the experimental one (Figure 8, *a*).

The phase boundaries shown in Figure 8, *b*, were determined based on the temperatures of the maxima of the dependencies

$$\Delta S(T, \Delta H) = S\big(T, H, Q_0^*(H, T), y^*(H, T)\big) - S\big(T, 0, Q_0^*(0, T), y^*(0, T)\big).$$

$T_{\max} = T_N$ and the line $T_N(P)$ corresponds to the spontaneous transition line for $\Delta S^m h, c(T_{\max})$ $\big(y^*(T_{\max}) = 0\big)$, as follows from the inset in Figure 8, *b* regardless of the magnitude of the external field H at which the magnetization is measured. Thus, the experimental measurements $\Delta S^m h, c(T_{\max})$ for a given interval of magnetic field changes ΔH by Maxwell's method for phase transitions of the 2nd order allow u determining the critical temperature of the phase transition of the 2nd order in an external magnetic field.

Under pressure, the character of magnetic ordering can change from the isostructural transition of the 2nd order PMorth−HMorth observed at $P < 4$ kbar to the blurred magnetostructural transition of the 1st order PMhex $\leftrightarrow$ HMorth, at $P > 4$ kbar, e. g., at 8 kbar (see Figure 9).

Analysis of Figure 8 and Figure 9 shows that the baric lowering of the characteristic temperatures of the structural transition of the 1st order (see Figure 8) eventually leads

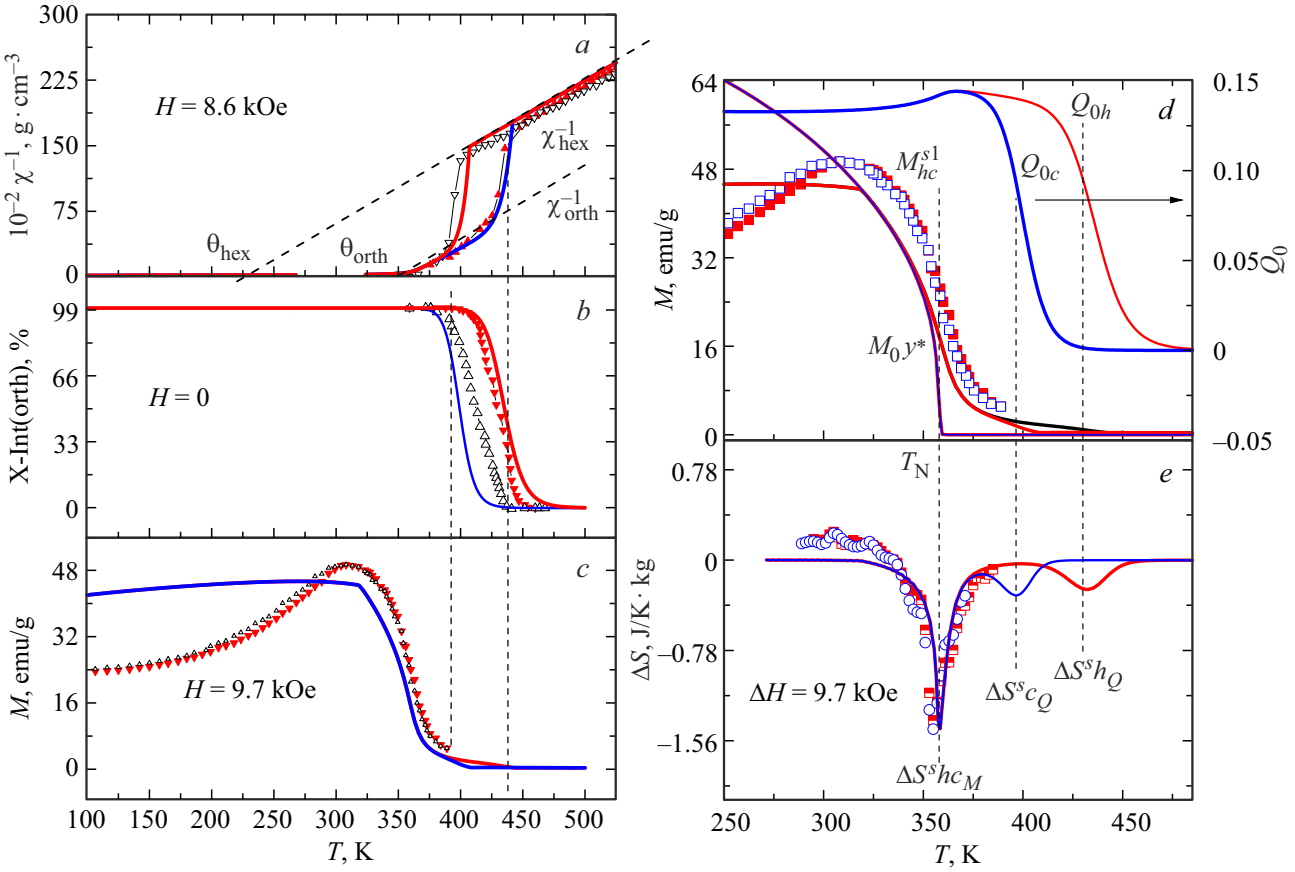


Figure 7. Combined experimental [3,4,10] (symbols) and theoretical (lines) temperature dependences of magnetostructural characteristics at atmospheric pressure. Model dependences are calculated for $g = 190$. Hereafter, blue (c)/red (h) curves correspond to cooling/heating; light/dark symbols correspond to cooling/heating. The curves M_0y^* define renormalized temperature dependences of the order parameter at $H = 0$ (Figure 7, d); Neel's temperature $T_N \approx \theta_{orth}$ is determined from the condition $M_0y^*(T_N) = 0$; splitting of the model magnetization dependence $M(T)$ (Figure 7, c and 7, d) in the structural transition region (dashed vertical lines) determines the anomalous splitting of the inverse susceptibility into 2 branches $\chi_{hex}(T)^{-1}$ and $\chi_{orth}(T)^{-1}$(Figure 7, a).

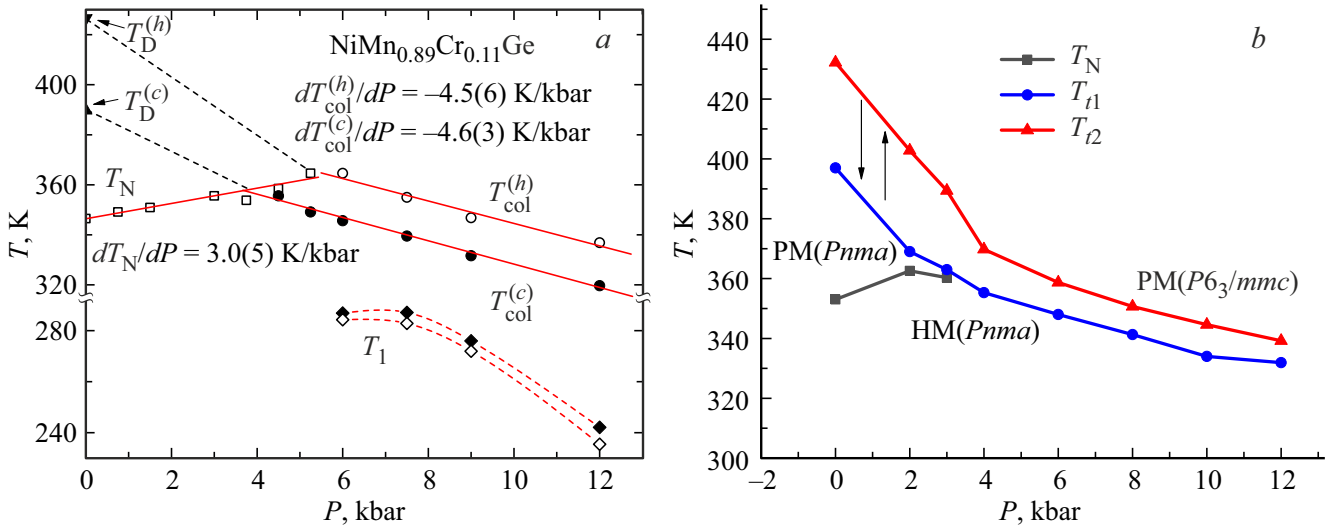


Figure 8. Experimental [13] (a) and theoretical (b) phase $P-T$-diagram of a slowly cooled $Mn_{0.89}Cr_{0.11}NiGe$ sample. The inset gives the temperatures of the maxima $\Delta S(T)$ and the feature temperatures of the magnetic and structural order parameters.

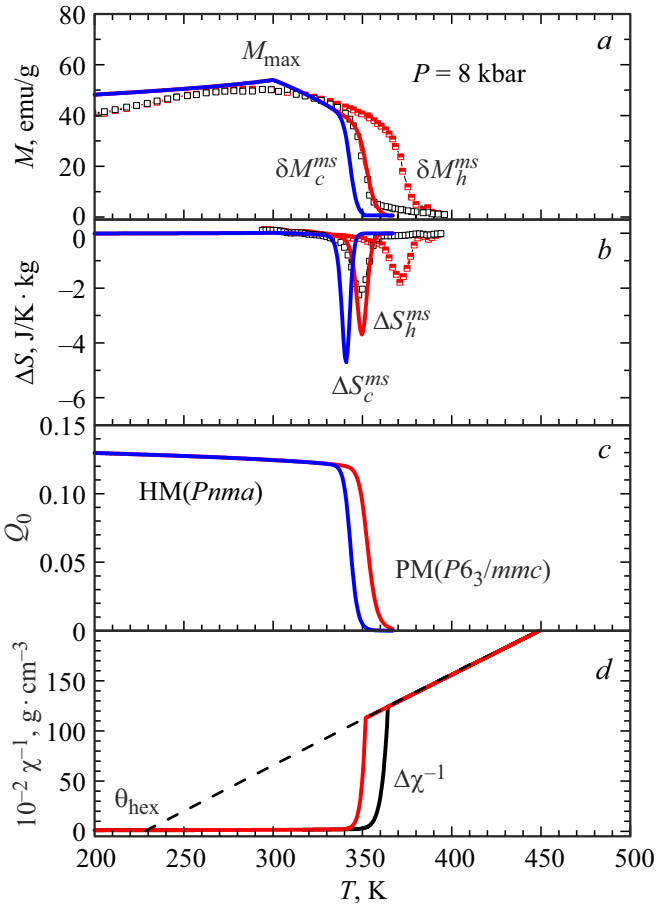


Figure 9. Pressure-stimulated blurred magnetostructural transitions of the 1st order in a slowly cooled sample. Symbols — experiment [2], lines — model.

to the appearance of a single magnetostructural transition accompanied by the synchronous appearance of the parameters of the structural (Figure 9, c) and magnetic (Figure 9, a) order. A similar situation occurs when the samples are quenched, but there are significant differences.

We will simulate the effect of quenching in this study by increasing the intracellular interaction parameter ω. 3 values of this parameter are provided in Table 2. The first value is used to describe the magnetic, structural, and magnetocaloric properties of slowly cooled images. Two further values are used to describe the properties of two independently prepared rapidly quenched samples with differing temperatures of blurred magnetostructural transitions of the 1st order. The associated parameters for each of the values of ω will be the parameters $A, \tilde{A}, B, \tilde{B}$, (A8d) and T_0. Each increase of the parameter is accompanied by such an increase of the parameter A that the cosine of the angle Ψ ($\cos(\Psi)$) between the resulting magnetic moments of the nearest planes perpendicular to the wave vector of the helimagnetic structure $\mathbf{q}[0, 0, q_a]$. The decreasing parameter T_0 describes the decreasing magnitude of θ_{hex} in each of the independent rapidly quenched samples.

The results of the calculations shown in Figure 10 and Figure 11 give an indication of the acceptability of the model assumptions used to describe the apparent and non-obvious properties of the quenched specimens. Thus, the successive increase in the values of $\sqrt{N_0}\omega$ from 4.284 for slowly quenched samples (Figure 7, Figure 9) to 6.426 and further to 7.283 to describe the properties of rapidly quenched samples (Figure 10 and Figure 11) leads to the superposition of structural and magnetic transitions into single blurred magnetostructural transitions of the 1st order with lower characteristic temperatures. These processes are accompanied by an increase in magnetic and magnetocaloric characteristics with a significant decrease in the values of $\Delta\chi^{-1}$ at $T = T_N$ (Figure 9) and structural order parameters Q_0. Analysis of the equations of state for the magnetic and structural order parameters $(\partial\Omega/\partial Q_0) = 0$, $(\partial\Omega/\partial y) = 0$ shows that in the considered approach the occurrence of the magnetostructural transition is induced by the spin subsystem. Since the temperature T_{t1} of the spontaneous ($y = H = 0$) occurrence of the structural order parameter Q_0 becomes negative for selected values of ω, ν_0. Therefore, the emergence of orthorhombic structure is only possible if magnetic order occurs simultaneously. It is suggested that such a combination of energetic parameters

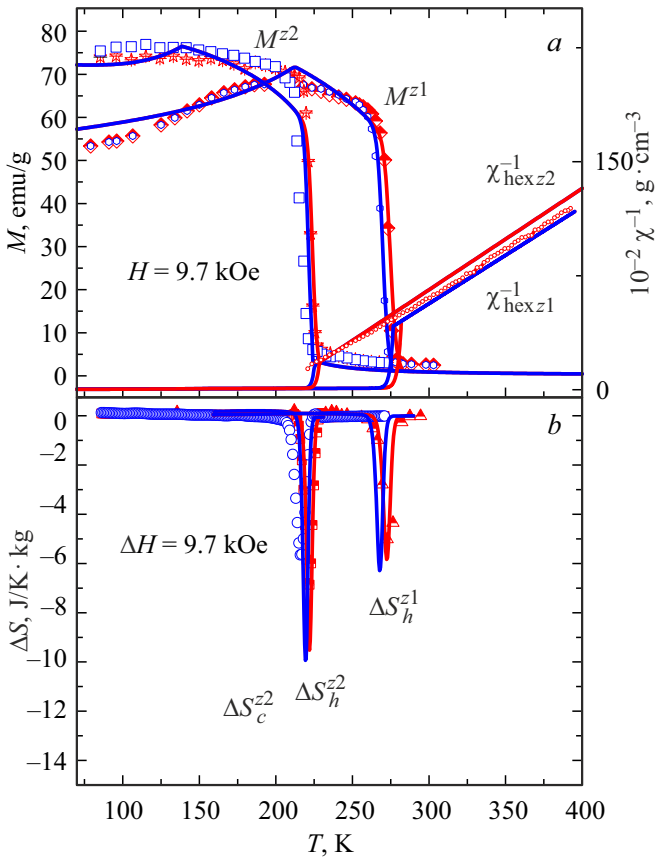


Figure 10. Temperature dependences of magnetic and magnetocaloric characteristics of quenched samples at atmospheric pressure. Symbols — experiment; lines — model.

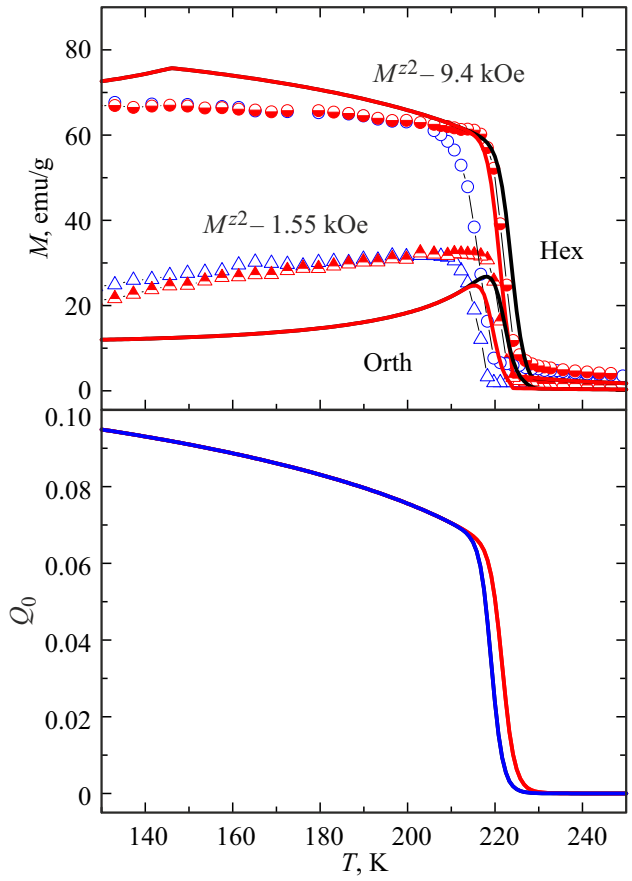


Figure 11. Temperature dependences of the magnetostructural characteristics of a quenched sample № 2 in magnetic fields of different strengths. Symbols — experiment; lines — model.

arises from the rapid freezing of the metastable distribution configurations of Mn and Ge atoms. The variety of such configurations, which differ in the degree of randomness in the population of atomic positions, can lead to a scatter of characteristic temperatures and magnetocaloric characteristics of rapidly quenched samples. This can be accounted for in theoretical description by using different values of the control parameters Ω, A, B, T_0.

It should be noted that this result is not related to the reduction of the lattice cell volume, which is a prerequisite for the baric transformation of the isostructural transition of the 2nd order into a magnetostructural transition of the 1st order.

6. Conclusion

Preliminary analysis of the measurements made on the quenched specimens shows that the main effects of quenching are summarized into three results.

1) Alignment of the blurred structural transition of the 1st order PMhex ↔ PMorth and the isostructural magnetic transition of the 2nd order PMorth−HMorth into a single blurred magnetostructural transition of the 1st order PMhex ↔ HMorth.

2) Multiple increase of the magnetocaloric effect with decreasing characteristic temperatures of the magnetostructural transition.

3) Uncontrolled variation of characteristic magnetostructural transition temperatures for independently prepared and independently quenched samples.

The attempt to explain the effects of quenching by analogy with the effects of hydrostatic and chemical (increase in concentration x) pressure does not correspond to the realities. Indeed, on the one hand, both types of pressures can lead to a single magnetostructural transition of the 1st order with decreasing characteristic temperatures and increase of MCE [5,11]. However, a significant discrepancy between these analogies is uncovered when analyzing the X-ray diffraction results of quenched and slowly cooled samples.

Thus, it was found that in the slowly cooled sample, the baric stimulation of the appearance of a single magnetostructural transition of the 1st order PMhex ↔ HMorth is attributable to the convergence and overlap of magnetic and structural transitions as the pressure [2,11–13] increases and, accordingly, the compression of the initial lattice cell of the slowly cooled sample increases [5].

A completely different situation is observed in the quenched sample. According to the data in Ref. [14], the magnetostructural transition of the 1st order PMhex ↔ HMorth takes place in the quenched sample under such conditions when the initial (in the hexagonal phase) cell volume of the quenched sample) exceeds the initial cell volume of the slowly cooled sample at atmospheric pressure. Hence, the effect of quenching leading to the occurrence of the magnetostructural transition of the 1st order PMhex ↔ HMorth, cannot be analogized to baric action since there is no compression of the lattice cell.

We hypothesize that the quenching process of the samples and their subsequent magnetostructural properties are related to the freezing of high-temperature metastable configurations of the distribution of Ge and Ni atoms at their eigenpositions. At the same time, fluctuations in the initial quenching temperature and its rate can lead to freezing of metastable configurations with different distributions of Ge and Ni atoms at these positions. It implies the difference in the degree to which the positions of Ni atoms are filled with Ge atoms and, respectively, the positions of Ge atoms with Ni atoms. Conservation of the chemical composition for any of the metastable configurations does not lead to a change in the lattice cell volume, but presumably may be responsible for the lowering of the intercellular interaction energies of the structural subsystem responsible for the occurrence of the structural transition. This can lead to such a decrease in the characteristic temperatures of the structural transition that in the process of combining the structural and magnetic transitions will form a single magnetostructural transition of the 1st-order. In this case, the temperature of the single

transition can fluctuate depending on the fluctuations of the atomic distribution of the freezing configurations. This assumption does not contradict the following facts: at slow cooling of the sample from the homogenization temperature 850 °C, it is quite admissible that a stable configuration of atoms is realized in the structural subsystem, when Ge atoms occupy the Ge positions, and Ni atoms occupy the Ni positions. It is with this configuration, which is characteristic of slowly cooled samples, that the structural subsystem possesses the maximum structural transition temperature and the separation of the characteristic temperatures of the structural and magnetic transitions. Consequently, if a less stable configuration is frozen in the structural subsystem as a result of quenching, it is quite acceptable to assume a reduction in the stability region of the orthorhombic phase and a decrease in the structural transition temperature without compression of the original crystal cell.

Funding

The study was supported by the Ministry of Education and Science of the Russian Federation, budget topic „Fundamental and Applied Aspects of the Development of the Physics of Magnetic Phenomena in Correlated Systems“ FREZ-2023-0002 (V.I. Valkov, A.V. Golovchan, I.F. Gribanov, O.Ye. Kovalev, R.A. Safonov, N.Yu. Nyrkov) and Assignment 1.2.1 „Synthesis of new magnetic materials that are promising for the development of technical devices of a new generation“ subprogram „Condensed matter physics and the creation of new functional materials and technologies for their production “ (V.I. Mityuk, A.L. Zheludkevich).

Conflict of interest

The authors declare no conflict of interest.

Appendix

It is assumed that a structural subsystem consisting of N_0 elementary hexagonal cells can experience a structural transition of the 1st order $\mathrm{PMhex}(P6_3/mmc) \leftrightarrow \mathrm{PMorth}(Pnma)$. This transition is interpreted as a jump-like cooperative displacement of Ni and Ge atoms (see Figure 6) in all cells at a strictly defined temperature. This cooperativity arises from intercell interaction between local displacements in individual cells. We will hereafter refer to these transitions as point transitions of the 1st order.

To describe the thermodynamics of the structural transition $\mathrm{PMhex}(P6_3/mmc) \leftrightarrow \mathrm{PMorth}(Pnma)$ we use in the system $Mn_{1-x}Cr_xNiGe$ the Hamiltonian of the structural subsystem in the form of

$$H(Q_n) = \sum_n V(Q_n) - \frac{1}{2}\sum_{nn'} \nu_{nn'Q_nQ_{n'}}, \qquad \text{(A1)}$$

$$V(Q_n) = \frac{1}{2}\omega_0^2 Q_n^2 + \frac{1}{4}\gamma Q_n^4 + \frac{1}{6}\Gamma Q_n^6,$$

$$\omega_0^2 > 0, \quad \gamma > 0, \quad \Gamma > 0.$$

Here the variable $Q_n = Q_{nz}$ describes the group static displacements of the equilibrium positions for Ni atoms during stabilization of the orthorhombic phase. The statistical mean of this quantity $\langle Q_n \rangle$ is the structural order parameter; $V(Q_n)$ is the intracellular potential energy stabilizing the original hexagonal structure ($\langle Q_n \rangle = 0$). The presence of intercell interactions in the Hamiltonian $\nu_{nm}Q_nQ_{n'}$ under certain conditions can lead to cooperative displacements with $\langle Q_n \rangle > 0$ and stabilization of the orthorhombic phase $\mathrm{orth}(Pnma)$. The Hamiltonian of the magnetic subsystem ($\widehat{\mathbf{H}}_s$) and its coupling to the spin subsystem ($\widehat{\mathbf{H}}_{sQ}$) is accounted for in the following form:

$$\widehat{\mathbf{H}}_s = -\sum_{nk,n'k'} J_{nn'}^{kk'} \widehat{\mathbf{s}}_n^k \widehat{\mathbf{s}}_{n'}^{k'} - 2\mu_B \mathbf{H}_0 \sum_{nk} \widehat{\mathbf{s}}_n^k, \qquad \text{(A2)}$$

$$\widehat{\mathbf{H}}_{sQ} = -\sum_{nk,n'k'} \left[L_{nn'}^{kk'} Q_n Q_{n'} + L4_{nn'}^{kk'} (Q_n Q_{n'})^2\right] \widehat{\mathbf{s}}_n^k \widehat{\mathbf{s}}_{n'}^{k'}$$

$$\to -\sum_{nk,n'k'} \left[\widehat{\mathbf{s}}_n^k \widehat{\mathbf{s}}_{n'}^{k'}\right] \left\langle L_{nn'}^{kk'} Q_n Q_{n'} + L4_{nn'}^{kk'} (Q_n Q_{n'})^2 \right\rangle$$

$$-\sum_{nk,n'k'} \left\langle \widehat{\mathbf{s}}_n^k \widehat{\mathbf{s}}_{n'}^{k'} \right\rangle \left[L_{nn'}^{kk'} Q_n Q_{n'} + L4_{nn'}^{kk'} (Q_n Q_{n'})^2\right], \qquad \text{(A3)}$$

where $\widehat{\mathbf{s}}_n^k$ is the spin operator of the kth atom in nth hexagonal lattice cell; $J_{nn'}^{kk'} \equiv J_{nn'}^{kk'}(Q_0)$, $L_{nn'}^{kk'}$ is the energy parameters of effective spin-spin, spin-structure interactions, respectively $\mathbf{H}_0 = [0, 0, H_0]$ is the external magnetic field, μ_B is the Bohr magneton. The parameters $J_{nn'}^{kk'}(Q_0)$ and $L_{nn'}^{kk'}$ determine different types of relationship between the spin and structural subsystems.

The total thermodynamic potential of the system Ω is determined by the superposition of the TP of the spin Ω_s, structural Ω_Q and elastic subsystems Ω_e

$$\Omega = \Omega_s + \Omega_Q + \Omega_e. \qquad \text{(A4)}$$

The TP of the structural subsystem Ω_Q of N_0 structural units per unit volume is calculated in the shifted harmonic oscillator approximation (SHOA) and can be represented in the following form

$$\Omega_Q = U(Q_0, \sigma) - TS(T, \sigma), \qquad \text{(A5a)}$$

$$U(Q_0, \sigma) = N_0 \frac{\omega^2}{2}(Q_0^2 + \sigma) + N_0 \frac{\gamma}{4}(Q_0^4 + 6Q_0^2\sigma + 3\sigma^2)$$

$$+ N_0 \frac{\Gamma}{6}(Q_0^6 + 15Q_0^4\sigma + 45Q_0^2\sigma^2 + 15\sigma^3)$$

$$- \frac{1}{2} N_0 V_0(e_1, e_2) Q_0^2, \qquad \text{(A5b)}$$

$$S(T, \sigma) = \frac{N_0 k_B}{2} \ln \sigma(T), \qquad \text{(A5c)}$$

where k_B is the Boltzmann constant. The averages in the SHOA are calculated using the scheme

$$Q_0 = \langle Q_n \rangle_\rho = \int_{-\infty}^{\infty} \frac{1}{\sqrt{2\pi\tilde{\sigma}}} \exp\left[-\frac{(Q_n - Q_0)^2}{2\tilde{\sigma}}\right] Q_n dQ_n,$$

$$\sigma = \left\langle [Q_n - Q_0]^2 \right\rangle$$

and are treated as independent variable TP,

$$e_1 = e_{xx} + e_{yy} + e_{zz}$$

and

$$e_2 = (e_{xx} - e_{yy}) = (c/b - \sqrt{3})/\sqrt{3} \neq 0$$

elastic bulk and orthorhombic deformations of the lattice cell as a whole.

The thermodynamic potential of the spin subsystem Ω_s with helicoidal magnetic ordering is calculated in the mean space-periodic field approximation

$$\mathbf{h}_n^k = h\mathbf{U}_n^k \equiv h(\mathbf{q})\mathbf{U}_n^k(\mathbf{q}), \tag{A6a}$$

$$h(\mathbf{q}) = 2sy\left[J(\mathbf{q}) + 2LQ_0^2 + 2L4Q^4 - \Delta J(\mathbf{q})\cos^2(\vartheta)\right], \tag{A6b}$$

where $J(\mathbf{q}_a)$, L, $L4$ are the Fourier components of the effective spin-spin and exchange-structure interactions:

$$\begin{aligned} J(\mathbf{q}) \equiv J(q_a) &= \sum_{\Delta\mathbf{R}} J(|\Delta\mathbf{R}|)\cos(\mathbf{q}\Delta\mathbf{R}) \approx J_0(Q_0, e_1) \\ &+ J_1(Q_0, e_1)\cos(\Psi) + J_2(Q_0, e_1)\cos(2\Psi) \\ &= J_0(Q_0, e_1) + (2\delta^2 + 1)|J_2(Q_0, e_1)| \\ &= J_{00}\left[r_{AF} + |Q_0|^{2d}(\lambda_{AF} + \lambda_{1AF}e_1)2\right], \end{aligned} \tag{A7a}$$

$$\begin{aligned} \Delta J(\mathbf{q}) = J(\mathbf{q}) - J(\mathbf{q}=0) &= J_{00}\left[1 + 2|Q_0|^{2d}(\lambda_{20} + \lambda_{21}e_1)\right] \\ &\times 2z\left(\cos(\Psi) - 1\right)\left(2\delta(Q_0) - \cos(\Psi) - 1\right), \end{aligned} \tag{A7b}$$

where $\Psi = q_a c_{\text{hex}}/2$, $2\Psi = q_a c_{\text{hex}}$ are the parameters of the helicoidal structure described by the wave vector $\mathbf{q} = [0, 0, q_a]$, ϑ — angle between the direction of the local quantization axis $\mathbf{h}_n^k$ and the direction of the external field

$$\mathbf{H}_0 = [0, 0, H];$$

$$\mathbf{U}_n^k \equiv \mathbf{U}_n^k(\mathbf{q}) = \left[\cos(\mathbf{q}\mathbf{R}_n^k)\sin(\vartheta), \sin(\mathbf{q}\mathbf{R}_n^k)\sin(\vartheta), \cos(\vartheta)\right]$$

— unit vector defining the direction of the mean spatially periodic field (MSPF) $\mathbf{h} = h\mathbf{U}_n^k$, which is taken as the local quantization axis for the atomic spin operator $\hat{\mathbf{s}}_n^k$ at position $\mathbf{R}_n^k$ in the presence of an external magnetic field $\mathbf{H}_0$,

$$\langle \hat{\mathbf{s}}_n^k \rangle_h = \mathbf{U}_n^k \langle \hat{\mathbf{s}}_n^k \mathbf{U}_n^k \rangle_n = \mathbf{U}_n^k \langle \hat{m}_n^k \rangle_h = \mathbf{U}_n^k \langle \hat{m} \rangle_h = \mathbf{U}_n^k ys,$$

$$r_{AF} = 1 + K(\Psi, Q_0),$$

$$\lambda_{AF} = \lambda_{00} + \lambda_{20}K(\Psi, Q_0),\ \ \lambda_{1AF} = \lambda_{01} + \lambda_{21}K(\Psi, Q_0), \tag{A8a}$$

$$\lambda_{1AF} = \lambda_{04} + \lambda_{24}K(\Psi, Q_0),$$

$$J_{00} = J_0(Q_0 = e_1 = 0) = k_B T_0 2/3s(s+1); \tag{A8b}$$

$$K(\Psi, Q_0) = \frac{J_{20}}{J_{00}}\left(\cos(\Psi) - 1\right)[2\delta(Q_0) - \cos(\Psi) - 1],$$

$$\delta(Q_0) = -\frac{J_1(Q_0, e_1)}{4J_2(Q_0, e_1)}$$

$$\approx 1 - AQ_0^2 - \tilde{A}|Q_0|^{2d} + BQ_0^4 + \tilde{B}|Q_0|^{4d}; \tag{A8c}$$

$$J_2(Q_0, e_1) < 0, \quad J_1(Q_0, e_1) > 0. \tag{A8d}$$

The most effective competition between spin-spin $J_{0,2}(Q_0, e_1)$ and exchange-structure contributions (A3) in terms of the formation of $P-T$-diagrams occurs, according to Ref. [2], with the degree exponent in (A8d) $d = 5/9$. The mean values are calculated in MSPF according to the following scheme

$$\langle \hat{m} \rangle = ys = Sp\hat{m}e^{\beta h\hat{m}}/z(X) \equiv \sum_{m_s=-s}^{s} me^{\beta h m_s}/z(X), \tag{A9a}$$

$$z(X) = Spe^{\beta h\hat{m}} \equiv \sum_{m_s=-s}^{s} e^{\beta h m_s}; \quad X = -s/k_B T, \tag{A9b}$$

where $m \in -s, -s+1, \ldots, s$ is the eigenvalue of the projection of the spin operator $\hat{m} = \hat{\mathbf{s}}_n^k \mathbf{U}_n^k$ onto the mean-field direction $\mathbf{U}_n^k$.

The expression for the total nonequilibrium TP of a unit volume homogeneous system under pressure P with helicoidal magnetic ordering of spins s belonging to $N = 2(1-x)N_0$ atoms Mn in case of the approximations used can be reduced to the following form

$$\begin{aligned} \Omega &= ah_m(q_a, Q_0, e_1)y^2 - k_B NT \ln z(X) + U(Q_0, \sigma) \\ &- T\frac{k_B}{2}N_0 \ln(\sigma) + \frac{1}{2}e_1^2 k_0 + \frac{1}{2}k_1(e_2)^2 + Pe_1 - T(\nu_0 e_1), \\ ah_m &\equiv ah_m(Q_0, e_1) = NJ_{00}\left(J(q)/J_{00} - \Delta J(q)\cos\vartheta^2/J_{00}\right)s^2, \\ a &= NJ_{00}s^2 = (3/2)s^2 a_3 T_0/s(s+1)N = 2(1-x)N_0. \end{aligned} \tag{A10}$$

Equilibrium

$$y \equiv y(T),\ \ Q_0 \equiv Q_0(T),\ \ e_1 \equiv e_1[T, P, Q_0(T), y(T)],$$

$$e_2 \equiv e_2[Q_0(T)],\ \ \sigma \equiv \sigma[T, Q_0(T)],$$

ϑ are solutions of the equations of state at given values of pressure P and magnetic field H:

$$(\partial\Omega/\partial Q_0) = 0,\ \ (\partial\Omega/\partial y) = 0,\ \ (\partial\Omega/\partial\sigma) = 0,$$

$$(\partial\Omega/\partial e_1) = 0,\ \ (\partial\Omega/\partial e_2) = 0. \tag{11}$$

The first two equations, after substituting analytic expressions for the solutions, are reduced to species (A12) and solved numerically

$$(\partial\Omega/\partial Q_0) = 0, \tag{A12a}$$

$$y = B_s(X). \tag{A12b}$$

Here

$$B_s(X) = \left[\left(\frac{1}{2s+1}\right)\coth\frac{1}{2s+1}X - \left(\frac{1}{2s}\right)\coth\frac{1}{2s}X\right]$$

is the Brillouin function.

Equations $\partial J(q)/\partial q_a = 0$, $\partial\Omega/\partial\varphi = 0$, define the conditions for the existence of the helimagnetic structure with $H_0 = 0$ (A13a) and $H_0 > 0$ (A13b)

$$\cos\Psi = \begin{cases} \delta(Q_0) & \text{by } |\delta(Q_0)| < 1, \\ 1 & \text{otherwise,} \end{cases} \tag{A13a}$$

$$\cos\vartheta = \begin{cases} \dfrac{2H_0\mu_{\mathrm{B}}}{(J(q_a) - J(0))y} & \text{by } |\delta(Q_0)| < 1, \\ \dfrac{2H_0\mu_{\mathrm{B}}}{(J(q_a) - J(0))y} & \text{by } \left|\dfrac{2H_0\mu_{\mathrm{B}}}{(J(q_a) - J(0))y}\right| < 1, \\ 1 & \text{otherwise.} \end{cases} \tag{A13b}$$

The transition from the equilibrium solutions in the point model for the magnetic and structural order parameters follows the scheme (A11). To describe complex functions from these parameters, e. g., magnetization $M(T) = M_0 y\cos\big(\theta(T, H, y)\big)$, of the inverse susceptibility, etc., schemes could be utilized

1. $M^*(T) = M_0 y^*\cos\big(\theta(T, H, y^*)\big)$,

where $y^*_{c,h}(T) = y(T)L_{1c,h}(T)$.

2. $M^*_{c,h}(T)L_{1c,h}(T)$.

3. $\chi^{-1}_{c,h}(T) \equiv \chi^{-1}_{c,h}[y_{c,h}(T, H)$

$$= \frac{H_0}{M_{00}y\cos\big(\theta(T, H, y)\big)} \to \frac{H_0}{M_{00}y^*\cos\big(\theta(T, H, y^*)\big)},$$

where $L_{1c,h}(T)\left(1 + e^{\frac{\Delta U^{c,h}_{12}}{k_{\mathrm{B}}T}}\right)^{-1}$.

It is necessary to note that the strong influence of local spin fluctuations leads to an increase in the effective magnetic moment. Therefore, the fitting value $M_{00} > M_0$ (see Table 2) was used to describe the inverse susceptibility. These spin-fluctuation effects are not described within the model used, but are evident in transition metal alloys [15].

References

[1] I.F. Gribanov, A.V. Golovchan, V.D. Zaporozhets, V.I. Kamenev, L.D. Klishchenko, V.V. Koledov, V.I. Mityuk, A.P. Sivachenko. FTVD **28**, *3*, 13 (2018).

[2] V.I. Val.kov, I.F. Gribanov, E.P. Andreychenko, O.E. Kovalev, V.I. Mityuk. Physics of the Solid State **65**, *10*, 1683 (2023). https://journals.ioffe.ru/articles/57221

[3] V.I. Val'kov, A.V. Golovchan, O.E. Kovalev, N.Yu. Nirkov. FTVD **33**, *4*, 36 (2023). (in Russian).

[4] V.I. Valkov, A.V. Golovchan, I.F. Gribanov, O.E. Kovalev, V.I. Mitsiuk. Physics of the Solid State **66**, *6*, 956 (2024). https://journals.ioffe.ru/articles/58711

[5] A. Szytuta, S. Baran, T. Jaworska-Gota, M. Marzec, A. Deptuch, Yu. Tyvanchuk, B. Penc, A. Hoser, A. Sivachenko, V. Val'kov, V. Dyakonov, H. Szymczak. J. Alloys Compd. **726**, 978 (2017).

[6] B. Penc, A. Hoser, S. Baran, A. Szytuła. Phase Transit. **91**, 118 (2018).

[7] W. Bażela, A. Szytuła. Phys. Status Solidi A **64**, 45 (1981); W. Bażela, A. Szytuła, J. Todorović, A. Zięba. Phys. Status Solidi A **64**, 367 (1981).

[8] R. Blints, B. Zheksh. Segnetoelektriki i antisegnetoelektriki. Dinamika reshetki, Mir, M. (1975). (in Russian).

[9] V.I. Val.kov, A.V. Golovchan, V.V. Koledov, B.M. Todris, V.I. Mitsiuk. Physics of the Solid State **62**, 798 (2020).

[10] G.A. Malygin. UFN **71**, *2*, 187 (2001).

[11] V.I. Valkov, A.V. Golovchan, I.F. Gribanov, B.M. Todris, E.P. Andreychenko, V.I. Mityuk, A.V. Mashirov. Physics of the Solid State **65**, 276 (2023).

[12] V.I. Valkov, B.M. Todris, A.V. Golovchan, V.I. Mityuk, A.V. Mashirov. FTVD **32**, *2*, 7 (2022). (in Russian).

[13] R. Duraj, A. Szytuła, T. Jaworska-Gołąb, A. Deptuch, Yu. Tyvanchuk, A. Sivachenko, V. Val'kov, V. Dyakonov. J. Alloys Compd. **741**, 449 (2018).

[14] T. Jaworska-Gołąb, S. Baran, R. Duraj, M. Marzec, V. Dyakonov, A. Sivachenko, Yu. Tyvanchuk, H. Szymczak, A. Szytuła. J. Magn. Magn. Mat. **385**, 1 (2015).

[15] T. Moriya. Spivoviye fluktuatsii v magnetikakh s kollektivizirovannymi elektronami. Mir, M. (1988). (in Russian).

Translated by A.Akhtyamov